Design of coreless PCB transformers for power and signal isolation in a modular ADC system for power quality data acquisition

Michael T. Carpenter and Mark A. H. Broadmeadow
School of Electrical Engineering and Computer Science
Queensland University of Technology
Brisbane, Australia
Email: michael.carpenter@student.qut.edu.au

***Abstract*—Available industrial energy meters offer high accuracy and reliability, but are typically expensive and low-bandwidth, making them poorly suited to multi-sensor data acquisition schemes and power quality analysis. An alternative measurement system is proposed in this paper that is highly modular, extensible and compact. To minimise cost, the device makes use of planar coreless PCB transformers to provide galvanic isolation for both power and data. Samples from multiple acquisition devices may be concentrated by a central processor before integration with existing host control systems. This paper focusses on the practical design and implementation of planar coreless PCB transformers to facilitate the module's isolated power, clock and data signal transfer. Calculations necessary to design coreless PCB transformers, and circuits designed for the transformer's practical application in the measurement module are presented. The designed transformer and each application circuit have been experimentally verified, with test data and conclusions made applicable to coreless PCB transformers in general.**

I. Introduction

Industrial energy users are currently limited to expensive and low-bandwidth energy usage data collection devices. Although such metering devices are well suited to high-accuracy, high-energy systems, they are poorly suited to modular, multi-sensor data collection schemes and power quality analysis. To facilitate industrial process refinement, fault detection, energy usage and power quality analysis, an isolated, low-cost, high-bandwidth data acquisition module (herein referred to as a DAQM) is proposed. Data from the network of distributed measurement modules will be concentrated by a central processor (such as an FPGA), with a microcontroller facilitating the data logging and integration into existing control systems or computer consoles.

For the isolation of digital data, opto-couplers are a popular solution for many low- to moderate-frequency systems, however, opto-couplers capable of reliable operation at more than a few megaertz are expensive. A relatively new method of signal isolation, the digital isolator, can operate at up to many tens of megahertz, however with a typical cost in the order of dollars (A$) per two-channel unit, their application in a low-cost device (such is the data acquisition module) is limited. For the isolation of low-voltage analogue signals, isolation amplifiers may be used, however, as with digital isolators, their high cost can be prohibitive.

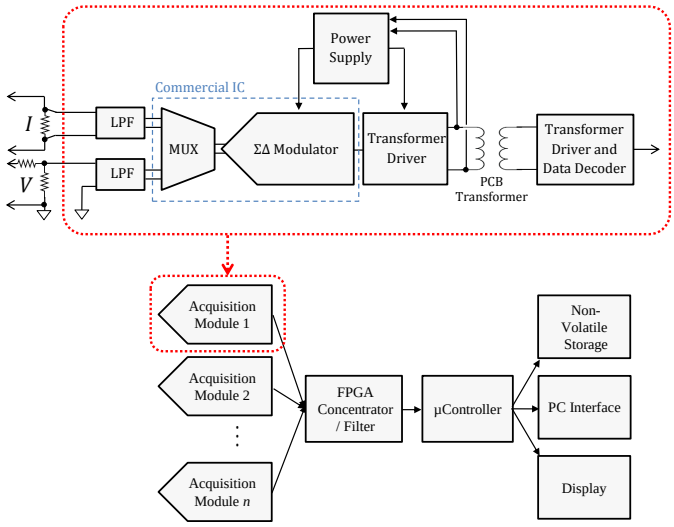

Fig. 1. Modular isolated power measurement system.

Considerable work has been published on the use of planar coreless PCB transformers in isolated gate drive circuits [1]–[4]. Although consumer inductive charging systems use a similar concept, coreless PCB transformers have not seen significant use as a power and signal transfer device within commercial electronics. Since a coreless PCB transformer's only cost is the PCB area it consumes, they are well suited for low-cost applications, and the use of standard PCB manufacturing processes makes their construction predictable and repeatable.

This paper focuses primarily on the practical application of planar coreless PCB transformers as used for the DAQM's isolated power, clock and data signal transfer. Calculations necessary to design the coreless PCB transformers are presented, and practical circuits intended for the DAQM application, but applicable to coreless PCB transformers in general, are included. The experimental validation section demonstrates the viability of the use of coreless PCB transformers (and associated circuitry) in the DAQM application.

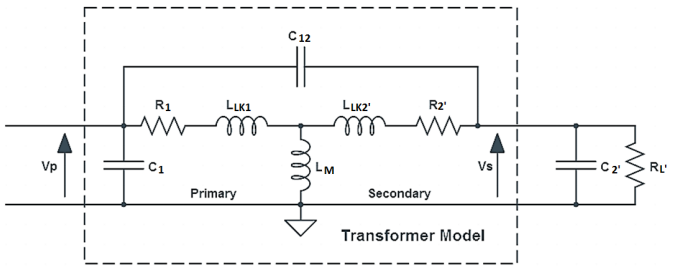

Fig. 2. High-frequency transformer model [1].

II. Proposed modular data acquisition system

The complete data acquisition system (figure 1) is comprised of several data acquisition modules (DAQMs), a data concentrator and filter FPGA, and a microcontroller attached to a PC, display and/or storage device.

The DAQM's analogue-to-digital conversion device is a commercial dual-input sigma-delta ($\Sigma\Delta$) modulator IC, with appropriate external signal conditioning to allow voltage measurement via a resistor divider, and current measurement via a shunt or current transformer (CT). This paper will refer to the data conversion side of the DAQM as the "secondary" side. The primary side of the DAQM consists of the coreless PCB transformer driver and data recovery circuitry. Isolated secondary-side power and the modulator's external clock signal are provided by a single planar coreless PCB transformer. This is teamed with a smaller, higher frequency coreless PCB transformer used to transfer measurement data from the sigma-delta modulator back to the host. For the selected modulator, the clock frequency will be approximately 8MHz, resulting in a data output rate of $f_{clock}/4$ (voltage and current multiplexed on one Manchester-encoded data stream) with a maximum input sampling rate of $f_{clock}/12$.

III. Planar coreless PCB transformers

The fundamental design of a planar coreless PCB transformer involves two planar copper spirals – one etched onto either side of a regular two (or more) layer PCB. The two windings are thus separated by the PCB's core (or prepreg), the material properties and thickness of which determine, to some extent, the transformer's performance and isolation voltage. The transformer's primary winding is then driven at high frequency, usually in the range of 2MHz to 20MHz in order to achieve either the maximum [input] impedance frequency (MIF; for low power systems) or the maximum efficiency frequency (MEF; for high power systems) [1]–[4]. [1] has demonstrated that an external secondary load capacitor, on the order of 100pF to 1nF, plays a significant role in the determination of the transformer's resonant frequency. In conventional coreless PCB transformer applications, the output voltage is then rectified and filtered, and efficiencies exceeding 90%, with a power density of up to 24W/cm^2 have been demonstrated [1].

A two-winding coreless PCB transformer may be described using the high-frequency transformer model in figure 2 [1], where:

R_1	Primary winding resistance;
R'_2	Secondary winding resistance, referred to primary;
R'_L	Load resistance, referred to primary;
L_{LK1}	Primary leakage inductance;
L'_{LK2}	Secondary leakage inductance, referred to primary;
L_M	Mutual inductance;
L_p	Primary self-inductance, equal to $L_M + L_{LK1}$;
L_s	Secondary self-inductance, equal to $L_M + L_{LK2}$;
C_{12}	Primary-to-secondary winding capacitance;
C_1	Sum of primary winding capacitance and primary driver output capacitance;
C'_2	Sum of secondary winding capacitance and external load capacitance, referred to primary;
n	Turns ratio;
μ_0	Permeability of vacuum;
a_1	Inner radius of ith circular track filament;
a_2	Outer radius of ith circular track filament;
h_1	Height of ith circular track filament;
r_1	Inner radius of jth circular track filament;
r_2	Outer radius of jth circular track filament;
h_2	Height of jth circular track filament;
z	Separation distance between the circular tracks;
$J_0(x)$	Bessel function of the first kind, order zero.

The self inductance of the planar winding [5] is given by

$$L_p = \sum_{j=1}^{N_p} \sum_{i=1}^{N_p} M_{ij} \tag{1}$$

$$L_s = \sum_{j=1}^{N_s} \sum_{i=1}^{N_s} M_{ij} \tag{2}$$

And thus, the mutual inductance between the two planar, multi-filament windings [5] may be represented as

$$L_M = \sum_{j=1}^{N_p} \sum_{i=1}^{N_s} M_{ij} \tag{3}$$

where the filament-to-filament mutual inductance, M_{ij}, has been reported in [5]

$$M_{ij} = \frac{\mu_0 \pi}{h_1 \ln(\frac{r_2}{r_1}) h_2 \ln(\frac{a_2}{a_1})} \int_0^\infty S(kr_2, kr_1) S(ka_2, ka_1) \, Q(kh_1, kh_2) e^{-k|z|} dk \tag{4}$$

where

$$S(kx, ky) = \frac{J_0(kx) - J_0(ky)}{k} \tag{5}$$

$$Q(kx, ky) = \begin{cases} \frac{2}{k^2}\left[\cosh k\frac{x+y}{2} - \cosh k\frac{x-y}{2}\right] & z > \frac{h_1+h_2}{2} \\ \frac{2}{k}\left[h + \frac{e^{-kh}-1}{k}\right] & z = 0, x = y = h \end{cases} \tag{6}$$

Note that $z = 0$ for the calculation of self-inductances. To approximate the performance of the coreless PCB transformer, [1] gives the resonant frequency as

$$f_0 = \frac{1}{2\pi\sqrt{L_{eq} C_{eq}}}; \tag{7}$$

and the s-domain voltage gain (8) and input impedance (9) as

$$\frac{V_s}{V_p} = G(s) = B = \frac{\frac{1}{X_1} + sC'_{12}Y_1}{nY}; \tag{8}$$

$$Z_{in} = \frac{1}{sC'_{12}(1-nB) + \frac{1-A}{X_1} + sC'_1}. \quad (9)$$

Although not of great concern in the DAQM application (due to the low secondary power requirements), the coreless PCB transformer's efficiency [1] may be calculated as

$$P_{out} = \frac{|G(s)|^2 \cdot |V_p|^2}{R_L}; \quad (10)$$

$$P_{in} = |V_p|^2 \cdot \Re\left[\frac{1}{Z_{in}}\right]; \quad (11)$$

and thus,

$$\eta = \frac{|G(s)|^2}{R_L \cdot \Re\left[\frac{1}{Z_{in}}\right]} \times 100\%. \quad (12)$$

Where

$$\begin{aligned}
L_{eq} &= L'_{LK2} + L_{LK1}||L_M \\
C_{eq} &= C'_2 + C'_{12} \\
R'_2 &= n^2 R_2 \\
L'_{LK2} &= n^2 L_{LK2} \\
C'_1 &= C_1 + \frac{n-1}{n} C_{12} \\
C'_2 &= \frac{1}{n^2} C_2 + \frac{1-n}{n^2} C_{12} \\
C'_{12} &= \frac{1}{n} C_{12} \\
X_1 &= R_1 + sL_{LK1} \\
X_2 &= R'_2 + sL'_{LK2} \\
Y_1 &= X_2[\frac{1}{X_1} + \frac{1}{sL_M}] + 1 \\
Y_2 &= \frac{1}{X_2} + sC'_{12} + sC'_2 + \frac{1}{n^2 R_L} \\
Y &= -\frac{1}{X_2} + Y_1 Y_2 \\
A &= \frac{sC'_{12} + \frac{X_2}{X_1} Y_2}{Y}.
\end{aligned}$$

IV. Implementation of Power and Signal Isolation using PCB Transformers

A. Power

The most basic use for a planar coreless PCB transformer is in an isolated power transfer application. Typically, this is achieved by driving the transformer at its maximum efficiency frequency (MEF) for high power transfer applications, or, where minimal power consumption is desired, the maximum impedance frequency (MIF). The MEF will tend to approach the MIF as the load current decreases [1]. Due to the low secondary load current of the DAQM, approximately 6mA at 3.3V (20mW), the MEF of the module's coreless PCB transformer was initially assumed to be equal to the MIF.

In most papers discussing planar coreless PCB transformers, the primary winding is driven in either a single-ended or bipolar manner (figure 3) with a relatively high supply voltage (12V being a common choice). The DAQM is instead designed to accommodate a single 3.3V supply, and hence, the PCB transformer was driven in a bipolar manner to achieve an effective doubling of the primary drive voltage. The primary drive circuit uses a simple relaxation oscillator for the resonant frequency generation, and the transformer's winding is driven directly by the Schmitt-trigger's high-current (±50mA maximum) push-pull outputs (figure 4).

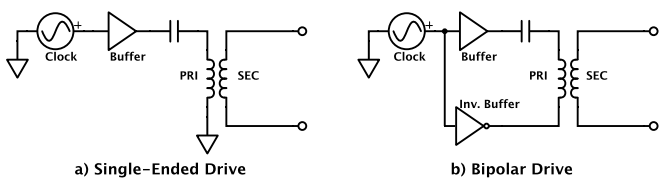

Fig. 3. (a) Single-ended and (b) bipolar transformer drive concept.

On the transformer's secondary side, a voltage-doubler rectifier topology, with a zener clamping diode is employed. The additional load capacitance, primarily due to the rectifier diode array D2 and series coupling capacitor C4, may be estimated as the coupling capacitor in parallel with the sum of the two junction capacitances in D2. For the circuit shown in figure 4, the maximum additional capacitance is about 20pF, resulting in an expected resonant frequency shift of -10%.

B. Clock generation and recovery

In order to simplify the filtering, synchronisation and data concentration of a multi-module measurement system, it is desirable to allow the sigma-delta modulator to be externally clocked by the host. Since the clock frequency was to remain relatively fixed at 8MHz, the simplest method of transferring the signal to the DAQM's isolated side was to set the coreless PCB transformer's primary drive frequency to be equal to a power-of-two multiple of the desired clock frequency. Thus, the clock signal may be extracted by rectifying, filtering and dividing the transformer's secondary voltage waveform (figure 4).

C. Data recovery

The sigma-delta modulator encodes both voltage and current information into a single Manchester-encoded bitstream at a rate equal to $f_{clock}/4$ (typically 2MHz). To transfer this data back to the DAQM's non-isolated side, a second coreless PCB transformer was used. Since the data signal is not periodic in the way that the clock signal is, it was necessary to configure the data transformer for a very high resonant frequency, thus ensuring that only the square wave edges were coupled via the coil. To achieve this, the equations in Section III imply that either the number of primary and secondary turns should be decreased, and/or the external load capacitor may be reduced or removed.

Figure 5 shows the signal transformer and data recovery circuit. On the DAQM's isolated side, the data output of the modulator is capacitively coupled into the signal transformer, which is driven in a single-ended configuration. On the non-isolated side, the low-amplitude (50mV to 300mV) positive- and negative-going spikes, which represent the rising and falling edges of the data signal respectively, are first amplified by a bipolar junction transistor (BJT, Q1). The amplifier's output is then coupled into two more BJTs with necessary biasing

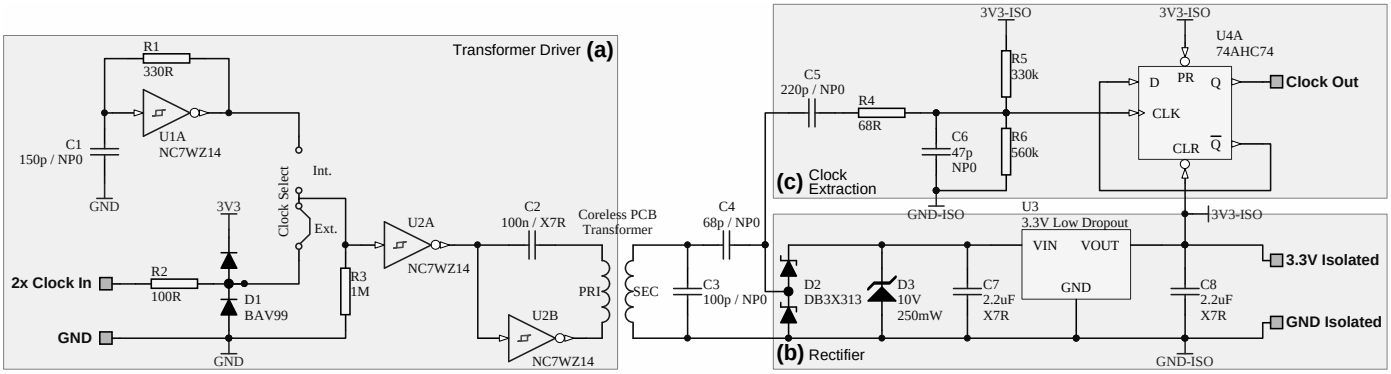

Fig. 4. Circuit schematic showing (a) coreless PCB transformer driver with (b) power rectifier and (c) clock extraction circuitry highlighted.

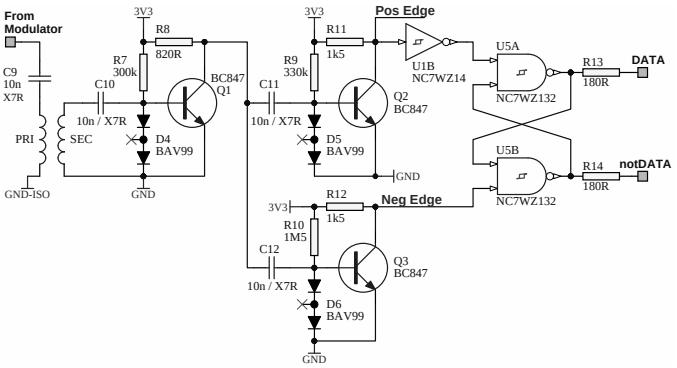

Fig. 5. Signal transformer and isolated data recovery circuit.

TABLE I. CALCULATED AND MEASURED EQUIVALENT CIRCUIT PARAMETERS FOR THE DESIGNED CORELESS PCB TRANSFORMER.

	Calculated	Measured	Error (%)
L_p	890.6nH	930nH	4.5%
L_{LK1}	418.5nH	465nH	10%
L_s	890.6nH	930nH	4.5%
L_{LK2}	418.5nH	465nH	10%
L_M	472.1nH	465nH	-1.5%

to allow the discrimination of the positive- and negative-going transitions (Q2 and Q3 respectively). A NAND-based set/reset latch with Schmitt-trigger inputs is then used to reconstruct the square waveform, with the complementary outputs allowing for differential signal driving back to the host.

V. EXPERIMENTAL VALIDATION

To validate the use of planar coreless PCB transformers in the data acquisition module design, a test PCB transformer was manufactured on a standard two-layer, 1.6mm PCB (figure 6). The transformer had 11 turns with identical primary and secondary windings, a track and spacing width equal to 254μm (10 mil), a 100pF external load capacitor (C3 in figure 4) and a 500Ω load resistor. With an outer diameter of 14mm and inner diameter of 2.8mm, the transformer's calculated and measured inductive parameters (200kHz test frequency) are shown in table I.

Figure 7 shows the test transformer's calculated and measured input impedance and voltage gain versus frequency,

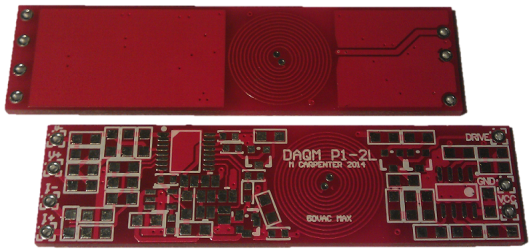

Fig. 6. Photograph of an initial unpopulated DAQM prototype with single 11-turn transformer.

where only the secondary-side load resistor of 500Ω is fitted (that is, no rectifier or clock decoder). The plots show a MEF (9dB voltage gain) at 18MHz and a MIF (142Ω input impedance) at about 14.5MHz (measured values). The calculated performance curves are shown to be a good representation of the actual device performance, especially with regard to the coreless PCB transformer's voltage gain.

A. Power

With the rectifier (no regulator; 500Ω load resistor) and clock extraction circuitry (figure 4) fitted, figure 8 shows the coreless PCB transformer's primary RMS drive current and rectifier output voltage versus frequency (at 3.3V drive voltage).

The figure shows a reduction in the maximum impedance and efficiency frequencies (14.5MHz and 18MHz to 13MHz and 15.5MHz respectively), most likely due to the additional load capacitance presented by the rectifier diodes. Whilst this frequency change can be predicted (as discussed prior) and accounted for by altering the load capacitor, in this case, the desired drive frequency is 16MHz and thus adjustment was not necessary.

The experimental data also demonstrate the effectiveness of driving the transformer in a bipolar manner, which has resulted in a maximum output voltage approximately 1.6 times the 3.3V primary supply voltage, thus increasing the usable voltage range of the module and simplifying the secondary voltage supply circuitry. Additionally, the wide frequency range for which the output voltage is adequate for 3.3V regulation may allow the transformer to be driven at a compromise frequency

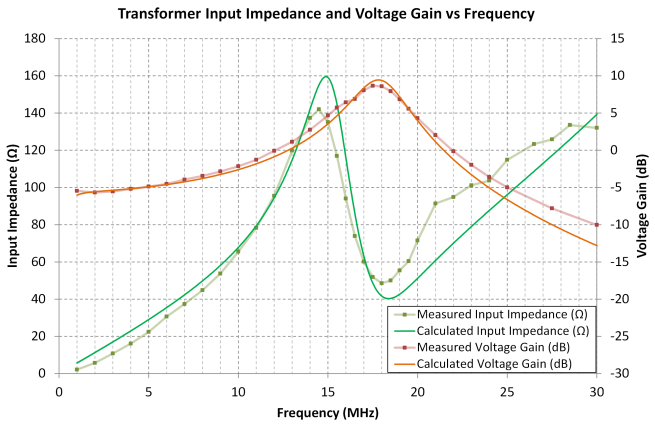

Fig. 7. Input impedance and voltage gain versus drive frequency, 500Ω load.

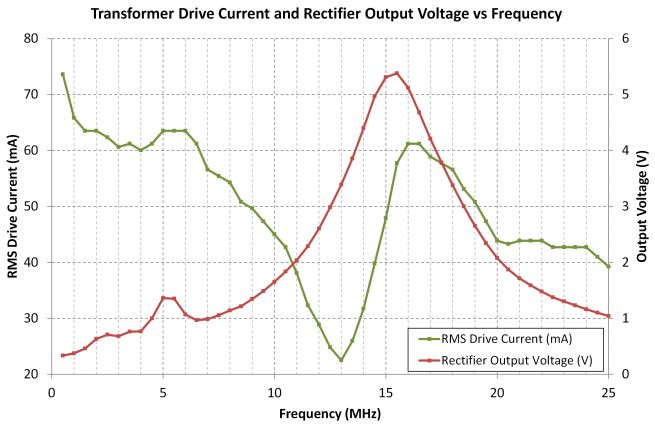

Fig. 8. Input impedance and output voltage versus frequency with 3.3V primary drive voltage, 500Ω load.

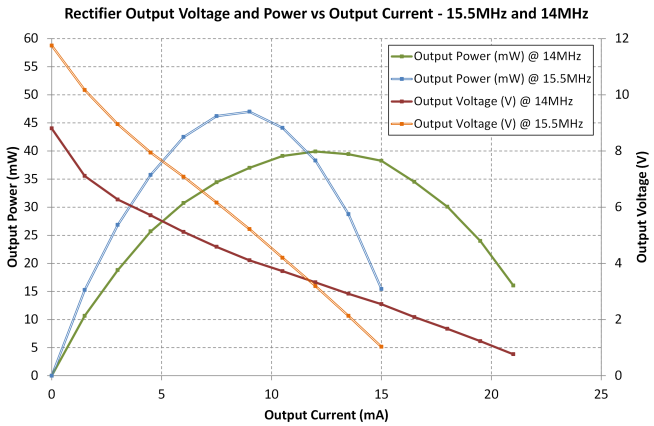

Fig. 9. Secondary output voltage and power versus load current at MEF (15.5MHz) and MIF-MEF compromise (14MHz) with 3.3V primary drive voltage.

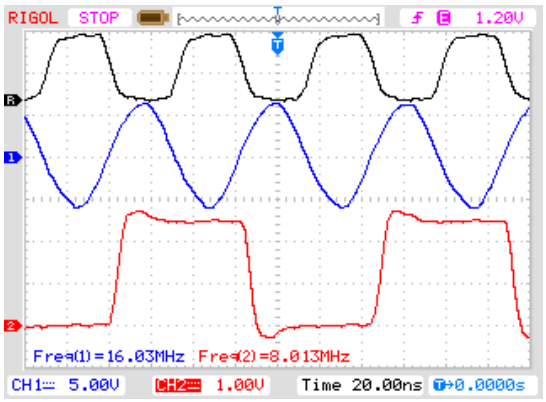

Fig. 10. 16MHz input clock signal (Reference, black); secondary output voltage (Ch. 1, blue); 8MHz extracted clock signal (Ch. 2, red).

between the MIF and MEF in order to reduce primary drive current.

Figure 9 shows the coreless PCB test transformer's secondary rectified output power and voltage versus load current, with a 3.3V drive frequency of 15.5MHz (MEF) and 14MHz (MIF-MEF compromise). It shows a maximum power point of 47mW when driving the transformer at its MEF, and that for a minimum pre-regulator voltage of 3.5V, the load current may be up to 11mA (about 40mW) – double the expected secondary power requirement. The data for the transformer at the MIF-MEF compromise (14MHz) show improved load regulation and a shift in the maximum power point toward greater load currents, although the maximum power is reduced by 15%. This suggests that transformer operation at a MIF-MEF compromise frequency (rather than at the MEF exactly) can have benefits for applications where the primary is driven by a current-limited source (such as the Schmitt trigger direct-drive circuit used in the DAQM design).

B. *Clock generation and recovery*

Since the sigma-delta modulator's clock is derived from the drive frequency of the primary winding, it is simplest for the drive frequency to be an exact power-of-two multiple of the desired modulator frequency, such that a series of D flip-flops may divide the signal down to the desired clock. Since the test coreless PCB transformer has been designed for a 16MHz resonant frequency (with prior figures showing this to be a good operating point in practice), a single flip-flop was used to extract the 8MHz signal. Figure 10 shows the 16MHz clock signal (Reference, black), secondary output voltage (Ch. 1, blue), and extracted clock signal (Ch. 2, red).

The divide-by-two clock extraction method appears effective, even with a varying secondary load, and further testing showed the simple circuit was able to accurately output a 50%-duty clock signal over the drive frequency range of 11MHz to 16MHz.

C. *Data recovery*

To asses the data recovery circuit, the test transformer's load capacitor (previously 100pF) was removed, such that the transformer's resonant frequency was much greater than the expected data frequency – a key requirement of the data transfer method. The decoding circuit was then tested by driving the transformer in a single-ended configuration with a simulated data source connected via a 10nF coupling capacitor (figure 5).

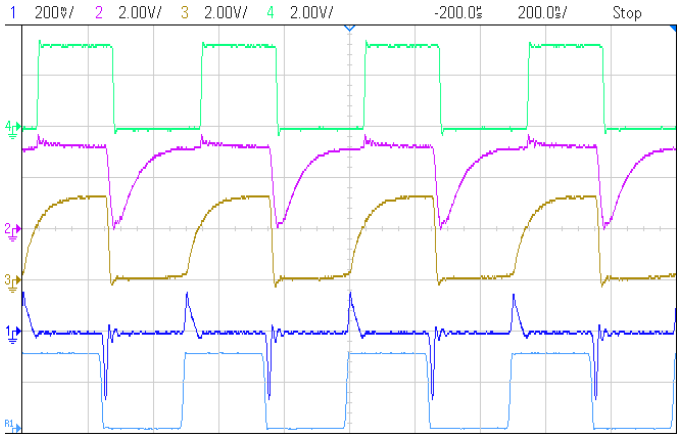

Fig. 11. Data into transformer (Reference 1, light blue); output of 5-turn transformer (Ch. 1, blue); output of negative edge amplifier (Ch. 2, magenta); output of positive edge amplifier (Ch. 3, yellow); recovered data signal (Ch. 4, green).

Since the data recovery circuit was capable of reliable operation with edge spikes of an amplitude as low as about 100mV, the 11-turn transformer was found to be excessive for the data signal transfer scheme. By cutting the PCB copper tracks on the primary and secondary side of the transformer, the performance of the data recovery circuit was tested using transformers consisting of five and three turns respectively. The test showed that for a 3.3V, 2MHz square wave input, the five-turn and three-turn transformers yielded edge spikes with amplitudes approximately 170mV and 50mV respectively.

Figure 11 shows the data recovery circuit operating at full-speed (2MHz), where Reference 1 (light blue) is the 3.3V, 2MHz simulated data into the 5-turn coreless PCB transformer's primary (which is on the DAQM's acquisition side); Channel 1 (blue) is the voltage at the transformer's secondary (on the DAQM's host-connected side); Channel 2 (magenta) is the output of the negative edge amplifier (node 'Neg Edge' in figure 5); Channel 3 (yellow) is the output of the positive edge amplifier (node 'Pos Edge' in 5); and Channel 4 (green) is the recovered 2MHz data signal.

Testing has demonstrated that the data recovery circuit is effective over a range of data rates and duty cycles, and that a coreless PCB transformer with as few as four to five turns can be expected to yield reliable performance at this data rate.

VI. Future work

The development of the coreless PCB transformer for use in the data acquisition module has yielded two key further research opportunities. With each module's coreless PCB transformer operating at 16MHz, significant electromagnetic interference (EMI), both radiated and conducted, may be expected. Whilst informal experimentation has shown that crosstalk between modules separated in-plane (i.e. placed side-by-side, the intended multi-module configuration) is much less than when the modules are stacked vertically, a thorough analysis has not yet been performed and thus the extent and effect of inter-module interference is not yet known.

[6] demonstrates that relatively thin (0.4mm) ferrite sheets can provide effective EMI shielding – up to a shielding effectiveness of 40dB for a bare ferrite sheet, or up to 60dB for the same sheet but with copper backing. Cost analysis has shown that such a ferrite sheet may increase the module cost by 10-20%, which may represent a worthwhile inclusion.

Other methods for EMI reduction include driving the coreless PCB transformer with a sinusoidal waveform rather than the square waveform used currently, and the possibility of using a spread-spectrum driver in order to reduce the amplitude of the fundamental drive frequency.

The second area of research interest involves the transmission of the data signal from the module's secondary side to the primary side, using the same coreless PCB transformer used to transfer the clock signal and provide isolated secondary power. This single-transformer concept is the ultimate goal of the DAQM's coreless PCB transformer design, with the original intention being that the data signal would be load- or resonant frequency-modulated at the secondary, resulting in detectable variations in the primary drive current. Such disturbance detection is performed in commercial RFID systems, where the receiver modulates its antenna's resonant frequency to allow the transmitter to identify the receiving device [7].

VII. Conclusion

The use of planar coreless PCB transformers has received some interest due to the advent of wireless inductive charging systems; however, such transformers have not seen significant use as a power and signal transfer device in commercial electronics. This paper presents the concept of a isolated, low-cost, modular data acquisition module designed for use in a distributed multi-sensor, single-host environment. Specifically, planar coreless PCB transformers are introduced and typical design processes and calculations are presented. The paper experimentally verified the viability of the use of the coreless transformers for the module's isolated power, clock and data signals. The experimental data presented are considered to be typical of a two-winding coreless PCB transformer, and the calculations and models may be used to represent any such coreless PCB transformer design.

References

[1] S. C. Tang, S. Y. Hui, and H. S. Chung, "Coreless planar printed-circuit-board (PCB) transformers - A fundamental concept for singal and energy transfer," in *Power Electronics, IEEE Transactions on*, vol. 15, no. 5, September 2000, pp. 931–941.

[2] ——, "A naturally soft-switched high-frequency gate drive circuit for power MOSFETs/IGBTs," in *Power Electronics and Drive Systems, IEEE International Conference on,*, July 1999, pp. 246–252.

[3] ——, "Optimal operation of coreless PCB transformer-isolated gate drive circuits with wide switching frequency range," in *Power Electronics, IEEE Transactions on*, vol. 14, no. 3, May 1999, pp. 506–514.

[4] ——, "Coreless PCB-based transformers for power MOSFET/IGBT gate drive circuits," in *IEEE Power Electronics Specialist Conference*, vol. 2, 1997, pp. 1171–1176.

[5] W. G. Hurley and M. C. Duffy, "Calculation of self and mutual impedances in planar magnetic substrates," in *Magnetics, IEEE Transactions on*, vol. 31, no. 4, July 1995, pp. 2416–2422.

[6] Y. P. Su, X. Liu, and S. Y. Hui, "Extended theory on the inductance calculation of planar spiral windings including the effect of double-layer electromagnetic shield," in *Power Electronics, IEEE Transactions on*, vol. 23, no. 4, July 2008, pp. 2052–2061.

[7] Y. Lee, "AN707: MCRF355/360 applications," pp. 1–3, 1999. [Online]. Available: http://ww1.microchip.com/downloads/en/AppNotes/00707a.pdf